

Journal of Materials Chemistry B

Accepted Manuscript



This is an *Accepted Manuscript*, which has been through the RSC Publishing peer review process and has been accepted for publication.

Accepted Manuscripts are published online shortly after acceptance, which is prior to technical editing, formatting and proof reading. This free service from RSC Publishing allows authors to make their results available to the community, in citable form, before publication of the edited article. This *Accepted Manuscript* will be replaced by the edited and formatted *Advance Article* as soon as this is available.

To cite this manuscript please use its permanent Digital Object Identifier (DOI®), which is identical for all formats of publication.

More information about *Accepted Manuscripts* can be found in the [Information for Authors](#).

Please note that technical editing may introduce minor changes to the text and/or graphics contained in the manuscript submitted by the author(s) which may alter content, and that the standard [Terms & Conditions](#) and the [ethical guidelines](#) that apply to the journal are still applicable. In no event shall the RSC be held responsible for any errors or omissions in these *Accepted Manuscript* manuscripts or any consequences arising from the use of any information contained in them.

Cite this: DOI: 10.1039/c0xx00000x

www.rsc.org/xxxxxx

ARTICLE TYPE

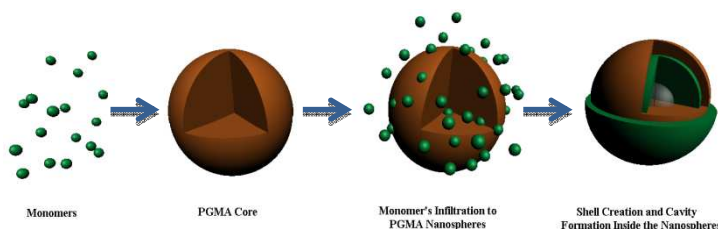
Microspheres as therapeutic delivery agents: Synthesis and Biological evaluation of pH responsiveness

C. Tapeinos, E.K. Efthimiadou*, N. Boukos, C.A. Charitidis, M. Koklioti and G. Kordas*

5 Received (in XXX, XXX) Xth XXXXXXXXXX 20XX, Accepted Xth XXXXXXXXXX 20XX
 DOI: 10.1039/b000000x

Abstract

A soft template method is used for the synthesis of pH responsive microcontainers with inner cavity. Poly Glycidyl Methacrylate (PGMA) microspheres of narrow size distribution are synthesized by soap-free
 10 radical emulsion polymerization and the coating of the microspheres is carried out with the same procedure. The procedure consists of two steps. In the first step the sacrificial template is synthesized and in the second step the shell is formed. Acrylic Acid is used as coating monomer aiming at introducing pH sensitivity in the synthesized microcontainers. Loading and Release study of the anthracycline drug DOXorubicin (DOX) is also carried out. The toxicity evaluation of the drug is studied by using the MTT
 15 assay and the necrotic effect was studied by Trypan Blue. Scheme 1 depicts the synthetic route of pH-Responsive microcontainers.



Scheme 1. Synthetic procedure of pH responsive microcontainers with inner cavity.

Keywords: Microspheres, Stimuli Responsive Microcontainers, Biological Evaluation

Introduction

Stimuli responsive nanocontainers attract great interest because of their application in drug delivery systems (DDS). A lot of research have been made lately in stimuli responsive systems
 25 using monomers such as Hydroxy propyl methacrylamide (HPMA) [1-4] and N-Isopropylacrylamide (NIPAAm) [5-7] that are thermo sensitive, Acrylic Acid and Methacrylic Acid which exhibit pH-sensitivity [8-11], Dimethyl amino ethyl methacrylate (DMAEMA) that exhibit thermo and pH sensitivity [8-10], and
 30 monomers with disulfide bonds such as N,N'-bis(2-oxopropanamide) bis(2-oxopropanamide) (Disulfide), that alternate their properties when found in a reductive-oxidizing environment. Exploiting the sensitivity of each monomer we can synthesize a smart DDS that will respond
 35 in each and every change in the external environment releasing the drug in a controlled manner. Core/Shell nanospheres and nanocontainers with stimuli responsive shell have extensively studied because of their potential use in medicine and especially in cancer treatment [1, 2, 10-28]. In this work poly(glycidyl
 40 methacrylate) (PGMA) microspheres of narrow size distribution

(400±20 nm as it can be seen by electron microscopy) were synthesized and used as template, and Acrylic Acid was used as the pH-sensitive coating monomer. Poly (Glycidyl Methacrylate) has also been used in the past for the synthesis of magnetic
 45 microspheres and microgels, using Free Soap Radical Emulsion or/and Atom Transfer Radical Polymerization [29-32]. Loading and release studies were carried out using DOXorubicin and a complete biological evaluation has been performed by using MTT assay in order to study the cytotoxicity of the final products,
 50 as well as Trypan Blue aiming at studying the necrotic effect on cells. A number of experimental techniques have been used for the characterization of the products. Scanning Electron Microscopy (SEM), Transmission Electron Microscopy (TEM) and Dynamic Light Scattering (DLS) were used to characterize
 55 the size and the morphology of the samples, Fourier-Transform Infra-Red Spectroscopy (FT-IR) and Raman Spectroscopy were used for the structural characterization, Ultra Violet Spectroscopy (UV) was used for the loading and release studies and Confocal Microscopy was used for the synthesis confirmation.

[View Online](#)

Experimental

Chemicals

Acrylic Acid (AA) was purchased from Sigma Aldrich and distilled before its use. Glycidyl Methacrylate (GMA) and Divinyl Benzene (DVB) were also purchased from Aldrich but used as received. Methyl Methacrylate (MMA) was purchased from Merck and was freshly distilled before its use and Potassium persulfate (KPS) was purchased from Panreac and used as received. Doxorubicin HCl (DOX) was provided by Pharmacia & Upjohn and used as received.

Characterizations

Scanning electron microscopy (SEM) and Transmission Electron Microscopy (TEM) images were obtained on an FEI Inspect microscope with W (Tungsten) filament operating at 25kV and an FEI CM20 microscope operating at 200kV respectively. Fourier transform infrared (FT-IR) spectra were obtained by a Perkin Elmer Spectrum 100 Spectrometer; the spectra were scanned over the range 4000-400 cm^{-1} . Raman Spectra were obtained with a Renishaw, inVia Raman Microscope. The dynamic light scattering (DLS) measurements were performed on a Malvern Instruments Zetasizer Nano Series, with a multipurpose titrator. In the data presented in this study, each measurement represents the average value of 3 measurements, with 11 to 15 runs for each measurement. UV-visible absorption spectra in the wavelength range of 200-800 nm were obtained on a Jasco V-650 spectrometer. An ultrasonic bath was used for sonication (Elma Sonic, S 30H). Confocal BioRad ,MRC 1024 ES.

Synthesis of monodisperse Polyglycidyl methacrylate (PGMA) seeds

PGMA seeds were synthesized by the emulsion polymerization method in a 250 ml glass spherical vial under nitrogen. In a typical procedure 175 ml of distilled water and 2.0 ml of GMA were added in the vial and the reaction vessel was purged with nitrogen for 40 min. The vessel was then heated to 80 °C and after that 200 mg of potassium persulfate (9.3 wt.% of the monomer; 5.0 ml water solution) was added as initiator. The reaction ended after 20 hours. The resulting product was separated by centrifugation and washed with water (3 times in 10000 rpm for 10 min each time).

Synthesis of PGMA@MMA-DVB-AA microcontainers

PGMA@MMA-DVB-AA microcontainers were fabricated as follows. 350 mg of PGMA microspheres were dispersed in 33 ml of distilled water in a 50 ml spherical glass vial and then placed in an ultrasonic bath for 40 minutes at 55 °C. After that the vial was transferred in a magnetic stirrer at 55 °C and agitated for 2 hours. Then the vessel heated at 80 °C and purged with nitrogen while 580 mg (617 μl) of MMA and 274 mg (300 μl) of DVB were added and agitated for an additional 1 hour. 68 mg (60 μl) of AA was slowly added and agitated 5 min before potassium persulfate (2.0 ml water solution) was added. The reaction ended after 18 hours and the product washed and collected by centrifugation (3 times in 7000 rpm for 5 min each time).

Determination of the -COOH entity

The carboxylic acid group entity was determined by the back-titration method. A weighted amount of the copolymer (30 mg)

was dissolved in 10 ml NaOH ($C = 0.1 \text{ M}$) and then the mixture was treated at 50 °C for 30 min aiming at reacting with the carboxylic acids. After this period, the excess of NaOH was back titrated with a standard solution of HCl ($C = 0.1 \text{ M}$) and phenolphthalein as indicator. The titration procedure repeated three times and the average volume of the hydrochloric solution was used for the COOH groups' determination. The mmol of COOH were determined according to the below equation:

$$n_{\text{COOH}} = n_{\text{NaOH}} - n_{\text{HCl}}$$

$$n_{\text{COOH}} = 0.25 \text{ mmol}$$

The carboxylic acid mmol that correspond to the amount of the polymer

$$n_{\text{COOH}} = 8.3 \mu\text{mol} / \text{mg of polymer}$$

Loading and Release study

The loading and release study of the synthesized microspheres were obtained through a standard method using Doxorubicin hydrochloride (DOX) as a model drug according to literature^[33]. 8.8 mg of hollow microcontainers were dispersed in 8.8 ml of PBS solution (Phosphate Buffer Saline, 10 mM) which has already been sterilized before its use. 2.1 mg of DOX was added, and the mixture was kept for 72 h under gentle agitation at 25 °C. After the above treatment, the sample was centrifuged (3 times at 12000 rpm and then washed again with water) aiming at removing the unloaded DOX. The same procedure for the drug encapsulation was followed in an isotonic solution (0.9 % NaCl). The loaded DOX was determined via ultra violet spectroscopy (UV), according to a standard curve which was prepared by making UV measurements in various DOX concentrations in a DOX/PBS solution using the PBS as a blank solution. The concentration of the loaded drug was calculated by, the difference of the concentration between, the original DOX solution and the supernatant, after loading. The examination of the release behaviour of DOX which was absorbed by hollow microspheres was investigated under different pH conditions. The different pH environments in which this study took place were either acidic (pH= 4, 10 mM, Citrate buffer) or slightly basic (pH=7.4, 10 mM, Phosphate Buffer Saline). The release study of DOX from the microcontainers was determined by dialysis. The DOX content in 1.0 mg/ml DOX-microcontainers is $391.3 \pm 0.5 \mu\text{g/ml}$. 1.0 mg of the DOX-loaded microcontainers was loaded into MWCO 140 KDa dialysis tube and dialyzed in a 10 ml either acidic or slightly basic buffer solution. At different time periods 1ml of the solution was removed and 1 ml of the respective buffer was added. The concentration of the released DOX was determined by absorbance measurements at 480 nm. Figure 8 depicts the percentage of the released amount, related to the total DOX concentration, as a function of time. The release experiments carried out at 25 and at 37 °C using a standard curve for each buffer solution.^[24, 27] Loading content and encapsulation efficiency were calculated by the equations below.

$$\text{Loading capacity \%} = \frac{\text{weight of the drug in microspheres}}{\text{total weight of the microspheres}} \times 100$$

$$\text{Encapsulation Efficiency \%} = \frac{\text{weight of the drug in microspheres}}{\text{weight of the feeding drug}} \times 100$$

Confocal study of Encapsulated substances

Encapsulation study was carried out using confocal microscopy, aiming at confirming the penetration of small molecules such as drugs (DOX), fluorescent molecules (FITC) and monomers, through microspheres' porous, for the polymerization in the inner of the seeds, after their swelling. Briefly, microspheres (10 mg) were stirring in an aqueous solution for two hours. Then the drug (2 mg) was added and the mixture left additionally for stirring, 48h in the dark. Subsequently the mixture centrifuged and the encapsulated microspheres froze dried. A similar way was used for FITC encapsulation. After the freeze-dry procedure, 5 mg of the solid, suspended in 0.5 ml of ethylene glycol and the mixture was deposited on a slide for confocal measurement.

Size and Polar Surface calculations via Molecular Simulation

Each molecule polar surface is calculated through ChemBio3D software. Based on the software we calculate the polar surfaces of each monomer and their size, based on the minimum energy conformation. The results (Size, polar surface and minimum energy) are presented in Table S1 (see supplementary info). In Fig. S4 (see supplementary info), confocal images of DOX and FITC encapsulated microspheres, are depicted. As it is observed, DOX and FITC, penetrate the lattice of the seeds through its porosity, therefore based on the fact that monomers and initiator's radicals are smaller than DOX and FITC, (table S1) we can conclude that the monomers can penetrate in the seeds porous also.

Cell Culture

MCF-7 (Human breast adenocarcinoma cells) cell line was maintained in DMEM supplemented with 10 % FBS, 2 mM l-glutamine, 100 units/mL penicillin and 100 g/mL streptomycin, were maintained in high glucose DMEM at 37 °C in 5% CO₂ atmosphere. 5 × 10⁵ Cells were seeded in a 96-well plate and after 24 h incubation, while in the exponential growth phase, they were treated with DOX, PGMA@MMA-DVB-AA and DOX encapsulated in PGMA@MMA-DVB-AA microspheres.

Cytotoxicity Assay by MTT

MTT assay was used aiming at investigating the cell viability after 48 h of incubation, of DOX, PGMA@MMA-DVB-AA and PGMA@MMA-DVB-AA-DOX in different concentrations. It is known that MTT is absorbed by mitochondria, where it is transformed into formazan by hydrogenase enzymes. Initially 5 × 10⁵ cells seeded in a 96 well plate and treated for 48 h with 10, 1, 0.1 and 0.01 μM of each compound and then incubated at 37 °C, 5% CO₂. Subsequently, MTT was added at a final concentration of 0.5 mg/ml, and the cells were incubated for additional 4 h at the same conditions, aiming at measuring the MTT (yellow) transformation into formazan crystals (purple) by the viable cells. The formazan crystals were solubilized for 4 h upon addition of DMSO and incubated at 37 °C. The absorbance of the lysate solution of each well was measured with a UV spectrometer at 550 nm (Reference wavelength 640 nm). The results from the MTT assay are presented based on the absorptions at 550 ± SD, using data of two different experiments (triplicate experiments).^[26-28]

Necrotic effects by Trypan Blue staining

MCF-7 cells, death or necrotic, were evaluated by the loss of cell integrity in their membrane using the trypan blue dye. Trypan blue dye broadly used to determine the loss of cell integrity, penetrates only the damaged cell's membrane and binds with the intracellular proteins inducing the blue staining of cells. For the trypan blue exclusion test, the total cells and the blue stained cells, which have been incubated with 0.4% (w/v) trypan blue for 5 min, were analysed by microscopy using a haemocytometer. Cells were incubated for 12, 24 and 48 h with 10 μM of DOX, either encapsulated or free, and the respective amount of the polymer which corresponds to the polymer that contains the above mentioned DOX concentration. Additionally, cells in the same concentration were used as a control. The cells (5 × 10⁵ cells/ml) were seeded in a 96-plate and the plate was left at 37 °C for 24 h aiming at an exponential growth phase. 50 μl of each cell suspension was diluted in 10× PBS and 18 μl of the solution were mixed with 2 μl of 0.4 % (w/v) of Trypan Blue. The results are presented as the concentration of Trypan blue+ve cells (n=2).^[27, 29]

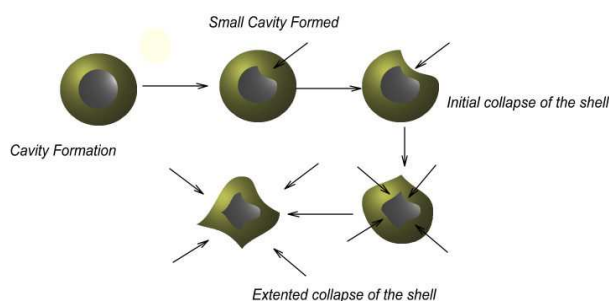
Results and Discussion

Synthesis

Synthesis of Poly (Glycidyl Methacrylate) microspheres was obtained following the procedure described in the experimental section. Free emulsion radical polymerization is one of the most simple, fast and economical way to polymerize a large variety of monomers. The polymerization mechanism of Glycidyl Methacrylate (GMA) is the same with the polymerization of Styrene and Methyl Methacrylate. A specific amount of a monomer is mixed with water under nitrogen atmosphere. Temperature increases to 80 °C and then the initiator is added. In 80 °C the initiator disintegrate giving free radicals. The free radicals react with the double bond of the monomers making them to break. As a result monomers start to merge leading to the final polymer. The spherical shape of the PGMA microspheres is due to the hydrophobicity of the polymer. It is noticeable that when polymerization starts, the solution pH is 5.5 but during polymerization pH drops to 3. In this acidic environment some of the epoxy rings of GMA may open and create hydroxyl groups that lead to hydrogen bonding between the microspheres. The coating procedure is also based on free radical emulsion polymerization. PGMA microspheres that were synthesized in the previous step are now used as a sacrificial template. The first step of the procedure is the treatment of the seed in the ultrasonic bath at 55 °C for 40 min. The aim of this is firstly to separate spheres between them and secondly to achieve swelling. The swelling property is enhanced through the two hours agitation in the magnetic stirrer at 55 °C. After 2 hours of agitating MMA and DVB are added and stirred for one hour more. The two hydrophobic monomers in their effort to avoid water solution infiltrate to the swelled PGMA seeds. When AA is added to the reaction system pH undergoes in a decrease from 5.5 to 2. PGMA seeds starts to hydrolyse and hydrogen bonds are created between the carboxylic group of the AA and the PGMA (AA has a pKa=4.35 and this means that is protonated below pH 4.35). After the addition of the initiator the polymerization starts, not only in the surface of the microspheres but in the interior too. The small molecules of the initiator penetrate through the pores of the microspheres, to the interior of the microspheres, and react with MMA and DVB monomers that are already there. Confocal microscopy was used to confirm the above mechanism. Fig. S4

[View Online](#)

(see supplementary info) presents the encapsulation of two molecules bigger than monomers and initiators (according to calculations on table S1 – see supplementary info) and this implies that smaller molecules will be encapsulated too. The cavity formation mechanism is described below in scheme 2. Polymerization takes place in the seed's surface and in the inner seed due to the fact that initiator radicals not only are absorbed in microsphere's surface but also penetrate the polymer lattice, creating that way, a polymeric shell. The internal polymerization starts with monomers that are already inside the seeds. As monomers polymerize they expand towards the edges of the microspheres. Because of the surface polymerization of MMA with DVB the cross linked shell becomes very stable preventing the internal polymers to expand further. During polymerization (acidic, pH=3) conditions the coherence of PGMA seeds is weakened due to hydrolysis, changing this way their morphology (Figure S5). This weakening helps in cavity formation which is not homeomorphous and this leads to shell collapsing in different areas creating the abnormal structure that can be seen in TEM.



Scheme 2. The mechanism of cavity formation

SEM and TEM Characterization

The size of the Poly (GMA) microspheres was 400 ± 20 nm (Fig. 1) but it could be controlled by changing the experimental conditions from 200 nm to some micrometres. The surface morphology can be seen in SEM and TEM images. It is obvious that the microspheres are not completely separated because of the hydrogen bonding that is created between them due to the hydrolysis of the epoxy ring of the microspheres and due to capillary forces which are developed in the reaction mixture and help by improving the inter-molecular interactions of the seeds between them and between other molecules (water and monomers). The surface is smooth and the sample is monodisperse. After a successful coating the morphology of the microspheres changes and the smooth spherical shape turns to an abnormal rough surface (Fig.2) with cavities. The cavities on the surface are a proof of an internal cavity that is formed due to experimental procedure as described by Lv et al and Zhang et al [34, 35]. TEM images show the created internal cavities of the microcontainers (Fig. 3).

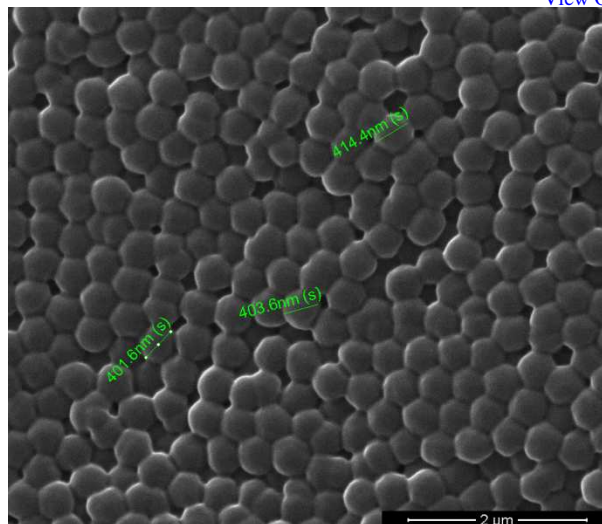


Figure 1. SEM image of PGMA microspheres

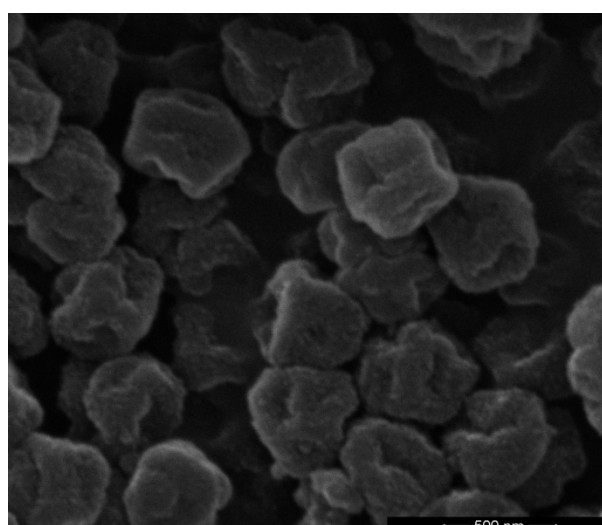


Figure 2. SEM image of PGMA microspheres coated with P(MMA – co – DVB – co – AA)

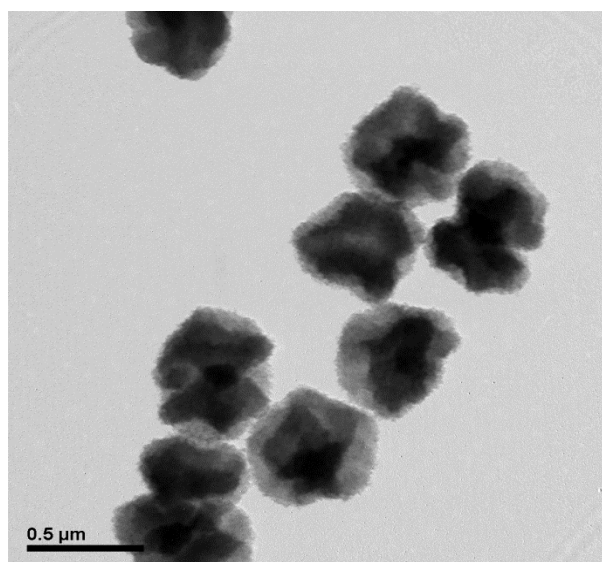


Figure 3. TEM images of PGMA@P(MMA – co – DVB – co – AA) microcontainers

IR Characterization

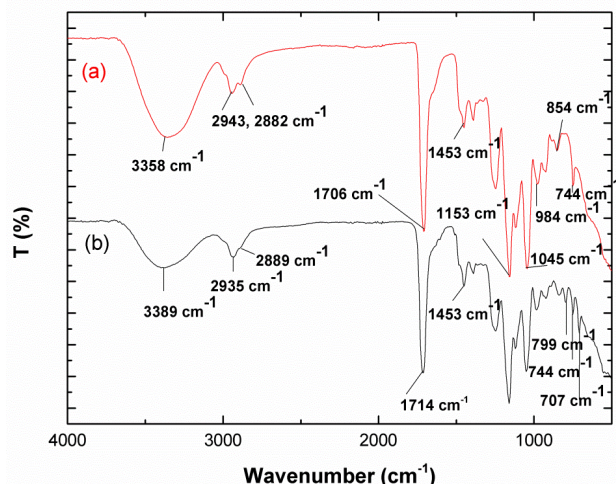


Figure 4. IR Spectra of (a) PGMA core microspheres and (b) PGMA@P(MMA-co-DVB-co-AA) shell

PGMA microspheres (Fig.4) present the characteristic C-H, bending vibration of epoxide ring at 744 cm^{-1} . The absorption peak of $1269\text{--}1153\text{ cm}^{-1}$ can be attributed to C-O stretching vibration in ester. Moreover, in the region of 1706 cm^{-1} the characteristic stretching of ester group is observed related to the carbonyl group of methacrylate segment ($\text{C}=\text{O}$). The FT-IR spectrum after the shell fabrication confirms the successful coating. From Fig. 4, it can be seen that there is a distinct absorption band from 1153 cm^{-1} to 1250 cm^{-1} , which can be attributed to the C-O-C stretching vibration of methacrylate. The two bands at 1388 cm^{-1} and 744 cm^{-1} can be attributed to the a-methyl group vibrations. The band at 984 cm^{-1} is the characteristic absorption vibration of PMMA, together with the bands at 1045 cm^{-1} and 854 cm^{-1} . The band at 1714 cm^{-1} shows the presence of the methacrylate carbonyl group. The band at 1453 cm^{-1} can be attributed to the bending vibration of the C-H bonds of the $-\text{CH}_3$ group. The two bands at 2943 cm^{-1} and 2882 cm^{-1} can be assigned to the C-H bond stretching vibrations of the $-\text{CH}_3$ and $-\text{CH}_2$ -groups, respectively. Furthermore, there are two weak absorption bands at 3358 cm^{-1} and 1641 cm^{-1} (Sh), which can be attributed to the $-\text{OH}$ group stretching and bending vibrations, respectively, of physisorbed moisture. On the basis of the above discussions, it can be concluded that the prepared polymer was indeed consists of PMMA [36]. The FT-IR spectrum of PGMA@P(MMA-co-DVB-co-AA) core shell microspheres (Fig. 2b) shows a peak at 799 cm^{-1} due to the vibration of phenyl group of DVB and carboxylic acid (AA) segment respectively. Due to the presence of both, the MMA and AA segment, the peak of each carbonyl group is overlapped and shifted at 1714 cm^{-1} . It is well known that the epoxy ring can be hydrolysed under acidic or basic conditions. The above mentioned hydrolysis it is possible to take place under the reaction conditions for shell fabrication. This hypothesis indicates through the vibration of C-O (of $-\text{OH}$ group) at the 3389 cm^{-1} region.

Raman characterization of loaded microcontainers

The Raman spectra of doxorubicin, PGMA@MMA-DVB-AA and PGMA@MMA-DVB-AA loaded with doxorubicin were obtained with a laser excitation wavelength of 785 nm . The bands observed at $300\text{--}500\text{ cm}^{-1}$ can be assigned to the encapsulation of the drug into the polymeric microparticles. Specifically, the peak

presented at 343 cm^{-1} can be attributed to the wagging vibration of C-O-H; at 446 and 463 cm^{-1} the peaks are due to the bending vibration of carbonyl group ($-\text{C}=\text{O}$) and the wagging vibration of C-OH of doxorubicin, respectively. [13, 37, 38] The weak band located at 918 cm^{-1} may be attributed to the epoxide asymmetric ring deformation of GMA. [37, 39] The intensity of this peak is linearly dependent on concentration of epoxy groups in the mixture. [40, 41]

The peak at 1000 cm^{-1} is assigned to the stretching vibration of C-O-C of PMMA and this peak is obvious in both spectra. [37, 42-44] Additionally, the peak at 1290 cm^{-1} may be assigned to hydrogen bonds of doxorubicin. [38] The band observed at 1575 cm^{-1} is interpreted by the (phenyl) ring vibration of doxorubicin [37, 38] and the bands which occur in the region $1608\text{--}1631\text{ cm}^{-1}$ are due to the stretching vibration benzene ring of DVB [37, 45]. The presence of carbonyl group from PMMA is confirmed by the band located at 1719 cm^{-1} . [43, 44] Finally, the bands at 2945 and 2998 cm^{-1} can be assigned to the characteristic symmetric and asymmetric stretching vibrations of $-\text{CH}_3$ and $-\text{CH}_2$ [37, 43, 44]

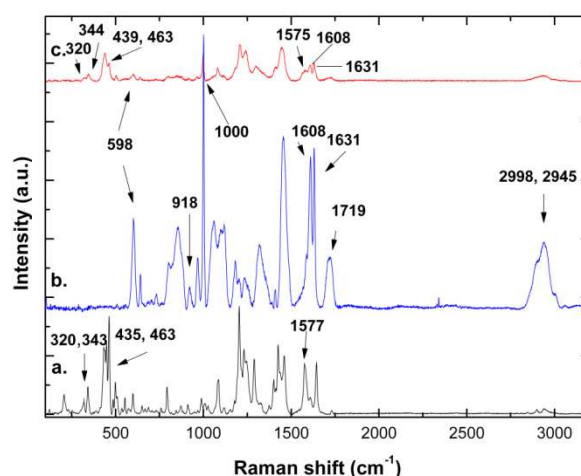


Figure 5. Raman Spectra of PGMA core microspheres and PGMA@P(MMA-co-DVB-co-AA) shell

DLS Characterization

From Dynamic Light Scattering measurements, we can acquire information about size distribution, dispersity and aggregation of the particles. The size depicted in the diagrams is a hydrodynamic parameter called z-average size and is comparable with size of other techniques, (i.e. electron microscopy) only when some conditions are satisfied. The conditions that have to be satisfied are that samples must be monomodal (i.e. only one peak), monodisperse, spherical or near spherical and have to be prepared in a suitable dispersant.

For our samples water is a suitable dispersant but they are of medium dispersity, bimodal (2 peaks) and near spherical so z-average size diverse from electron microscopy size measurements. In all diagrams, size is the mean z-average size of 5 measurements and concentration was chosen after DLS measurements of size versus concentration for five different concentrations (supplementary info, S1). In addition size versus time measurement was carried out (supplementary info, S2) in order to see if aggregation occurs when time passes. In figure 6(a) z-average size remains almost stable (600 nm) when pH ranges from 5 to 9 but when pH decreases under 5 then z-average sizes increases.

View Online

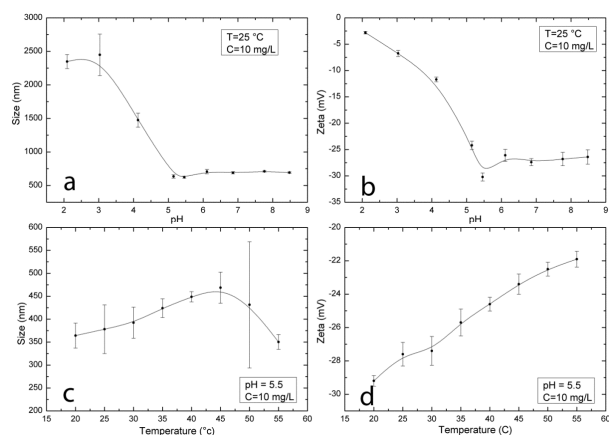


Figure 6. Size and Zeta Dependence Vs. pH & Temperature of PGMA microspheres

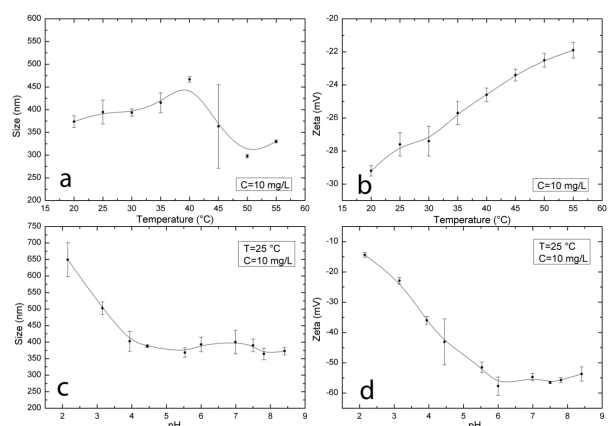


Figure 7. Size and Zeta Dependence vs. Temperature & pH of PGMA@P(MMA – co – DVB – co – AA) microcontainers

This happens due to hydrolysis of the epoxy group of Poly (Glycidyl Methacrylate). Hydrolysis lead to the formation of hydrogen bonds between the particles and aggregation occurs. Zeta potential (Fig. 6b) has almost a stable negative value between -25 and -30 mV at a pH range between 5 and 9 but becomes less negative as pH decreases. This behaviour can be attributed to the protonation of carboxyl groups. This decrement, supports size measurements results, because as zeta potential decreases solution becomes less stable and that can lead to aggregation. From size versus temperature diagram (Fig. 6c) z-average size increases from 360 nm (at 20 °C) to 450 nm (at 45 °C) and then decreases again to 350 nm (at 55 °C). This thermal response of Poly (Glycidyl Methacrylate) can be attributed to a possible swelling and de-swelling of the microspheres. In figure (6d) as temperature increases zeta potential decreases and this makes the colloidal system less stable.

In size and zeta potential versus temperature diagrams (Fig. 7a & 7b) a similar behaviour as in Poly (Glycidyl Methacrylate) is observed. This is due to the fact that shell coating isn't affected from temperature changes, so size alterations can be attributed to PGMA. As it concerns pH diagrams (Fig. 7c & 7d) things are different. Acrylic Acid is a pH sensitive monomer and this ability affects and it's polymer. When pH ranges from 4,5 to 9 size alterations are minor and we can see a big difference when pH is below 4,5. This is normal if we take into consideration that pKa of Acrylic Acid is 4.35 and this means that below this pH protonation of nanoparticles is

happening. Protonation results in a decrease on zeta potential because the negative charge from carboxyl groups decreases and furthermore results in aggregation of the microspheres because repulsive forces are weakened and hydrogen bonds between carboxyl groups are formatted.

Loading and Release

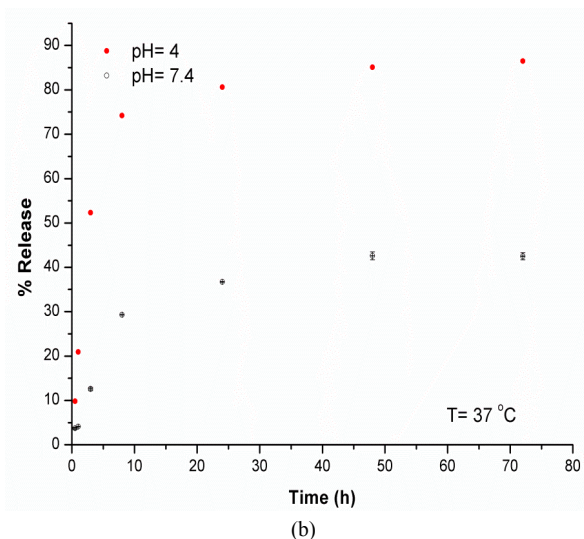
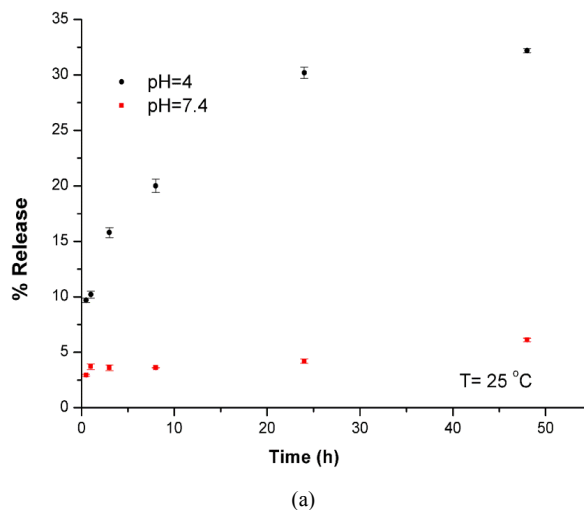


Figure 8. Doxorubicin released of PGMA@P(MMA – co – DVB – co – AA) microcontainers are studied at 25 °C (a) and 37 °C (b) at pH=4 and pH=7.4

The loading capacity of the synthesized microcontainers was examined under two different treatment solutions using the drug DOX. In the first case, the treatment solution was PBS. In these conditions the Loading Capacity (LC) was 39.1%, and the Encapsulation Efficiency (EE) was 78.8 %. In the second situation, we used as treatment solution an isotonic solution (NaCl 0.9 % w/v). The corresponding percentage in this case were low, LC=9% and EE=18%. As it is observed in Figure S3, the identical loading conditions are the ones in PBS solution, due to the fact that in pH=7.4, the DOX (pKa=8.2) is protonated and the microspheres are fully de-protonated (pKa= 4.3) resulting in enhancement of polymer – drug molecules interactions. Release study of synthesized microcontainers took place under different pH and temperature conditions. Figure 8a presents the release

study at 25 °C after treatment in acidic and slightly basic conditions. It is obvious that the drug release rate as well as the release percentage is higher at acidic pH. In the first 10 hours it is observed a 20 % release and then after 24 h the release reaches a plateau at 35 %. The major advantage is that at the above corresponding time (at slightly basic pH) the release percentage is about 8 %. A similar experiment carried out under treatment at 37 °C. The results of this study obviously present the drug release improvement. The release percentage after 10 h treatment is 50 % and finally, after 50 h the release percentage is 95 %. The corresponding percentage after 50 h incubation at 37 °C is 40 % at slightly basic conditions and after that time remains stable (Fig. 8b). The release results combined with the DLS measurements lead us to conclude that the synthesized microcontainers express a better behaviour at acidic pH in contrast to slightly basic pH.

It is well known that Doxorubicin (DOX) is one of the most important anthracycline antibiotic agents which widely used in cancer therapy and belongs to intercalation pharmacological group. Although its therapeutic efficacy, DOX presents many side effects such as cardio toxicity, myelo-suppression and multidrug resistance.^[46] Many research groups deal with improving these side effects through encapsulation of DOX in particular micro-carriers. Many studies about DOX encapsulation in micro-carriers such as liposomes^[46], micro particles^[47] or micelles^[33] refer that these systems can control drug release over extended periods of time, thereby increasing its efficacy and reducing toxic side effects. The drug association to polymeric systems can be either anionic or neutral, such as poly-acrylates *via* charge or hydrogen bonding interaction. In our case we have a polymeric system which consists of carboxylic acid groups (0.25 mmol / 33.2 mg of the polymer). The percentage of the PAA content is about 63.3 % (0.25 mmol × MW_{AA} = 21.03 mg, 21.03 mg / 33.2 mg = 63.3 % AA). Because of the anionic charged carboxylic groups (pKa = 4.5), cationic DOX (pKa = 7.6 at 37 °C and ionic strength 0.15) is high associated to the polymeric microspheres (EE = 78.8 % and LC = 39.1 %) ^[48]. This loading capacity, 391 ± 0.1 µg Dox/mg of polymer, is one of the highest according to literature. Carboxyl groups on the one hand, have the ability to form strong ionic interactions with desired drug candidates because they are excellent hydrogen bond donors. On the other hand anionic polymers, owing to their high negative-charge density they can bind substantial amounts of cationic drugs. Such an association based on ionic/electrostatic interactions is termed as polymer/drug complexation, and the complex formed is termed as polyelectrolyte complexes. As for the loading in isotonic solution, the possible mechanism is a salt mediation mechanism⁴⁹. In this kind of mechanism, DOX, in aqueous solution, without the addition of any other perturbation ions, develops repulsive interactions between DOX-DOX and between microcontainers which are greater than the cohesive interaction of microcontainers-DOX, and thus an insignificant amount of DOX can be absorbed by the microcontainers. After the NaCl addition (0.9% w/v), the increase of Cl⁻ ions may shift the balanced interactions toward the formation of DOX-microcontainers complexes because cationic DOX is also balanced with anionic Cl⁻ ions. Based on literature the low drug amount in loading procedure is attributed to the low amount of NaCl, and this enhances our indication about the possible loading mechanism (through electrostatic interactions). The release behaviour of the synthesized micro-particles can be explained by the drug pH-induced interactions. As it is observed in Figure 8a the drug's release rate from the polymer is better after treatment in acidic conditions than in slightly basic conditions. In this environment, in pH range 4.5 – 7.4 (pH_{pzc} DOX = 8.4 at 25 °C) electrostatic interactions are formed between ionized carboxyl

groups and NH₂ cation segment of DOX on the microspheres. Below pH 4.5 (at pH around 4) protonation of carboxylic acid segment led to the dissociation of the drug from the microcontainers surface. Above pH_{pzc}, PAA has almost completely ionized carboxyl groups and at pH = 7.4 in which DOX remain cationic charged, electrostatic interactions remain and only 10 % of the drug is released, possibly due to their absorption in the interior of the polymer microcontainers. At 37 °C, the drug dissociates more efficient than at 25 °C, due to the pKa value on this temperature^[50]. This release behaviour can be attributed to the drug solubility temperature dependence and also it is known that pKa depends on temperature and in the case of an exothermic reaction the equilibrium is moved from the protonated to the deprotonated drug improving that way the drug solubility. Taking into consideration that pKa value of Doxorubicin at 37 °C is 7.6^[51-55], in this pH a small percentage of the drug is anionic and as a consequence the drug is repelled from the polymeric microstructure. The remaining interactions now can be attributed at hydrogen bond formation.

Cell Viability

MTT assay

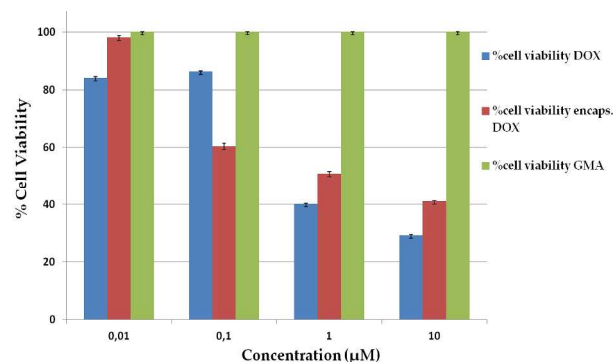


Figure 9. Cytotoxicity effect of Polymer (Green), DOX-loaded (Red) and DOX, against MCF7 breast cancer cells after 48 h treatment in different concentrations (±SD (n=3)).

MTT assay was used in order to investigate the cell viability after 48 h incubation of DOX and DOX-loaded microspheres, in different DOX concentrations (10 µM, 1 µM, 0.1 µM, 0.01 µM). In order to evaluate the contribution of the microspheres to the toxicity effect on MCF-7 cells we also investigate the cell viability of the unloaded microspheres (148, 1.48, 0.148, 0.0148 µg/ml of the microspheres quantities). The quantity of the unloaded microspheres that is used it's the same with the quantity of the polymer of the loaded microspheres if we remove from them the loaded drug. As it is observed in Figure 9, DOX exhibits toxicity at a high (10 µM) concentration and the toxicity decreases when the cells are incubated with lower DOX concentrations. As a result, the polymer is non toxic in contrast to encapsulated drug is toxic at a concentration of 10 µM corresponding to DOX. The above results are in good agreement with the biocompatible character of the polymeric structure.^[56,57]

Necrotic effect

MTT method evaluates quantitatively cell viability but cannot distinguish growth arrest or necrosis; Cell growth, as well as the percentage (%) of trypan blue +ve cells (necrosis) in the MCF7 cell line have been also studied. The necrotic effects of the Polymer (Blue), DOX-Polymer (Black) and DOX (Red) against

View Online

MCF7 breast cancer cells after 12, 24 & 48 h treatment in concentrations of 10 μM are presented in Figures 10 & 11. Figure 10, shows that after 12 h of incubation for DOX and the encapsulated DOX, the stained cells (dead cells) increased with time (24 h) (about 10 % in both cases) and after this time, the effect of DOX takes a plateau at 48 h.

Furthermore, the necrotic effect which is caused after the polymer treatment is irrelevant. Figure 11, confirms the above mentioned results and a similar behaviour is observed in the polymer. As a conclusion, trypan blue staining shows that treatment of the cells with free and encapsulated DOX generates a significant necrotic effect with time, despite the fact that the necrotic effect, which is caused from the polymer, is insignificant. This result is in good agreement with the MTT experiment because the toxicity which is induced from the polymer is meaningless.^[56,57]

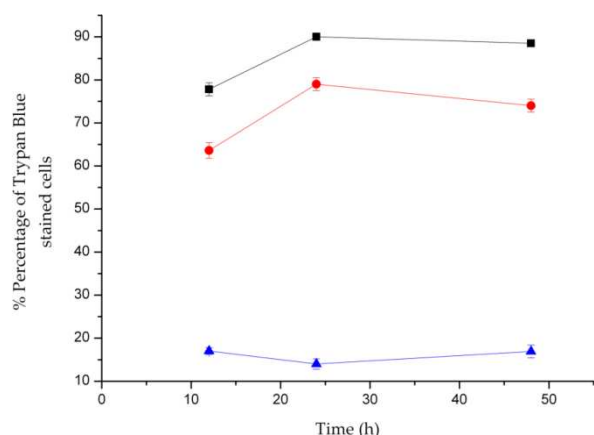


Figure 10. Treatment of MCF7 cells with Polymer (Blue), DOX-Polymer (Black) and DOX (Red), against MCF7 breast cancer cells after 12, 24 & 48 h treatment in 10 μM concentration and the respective amount of the polymer which corresponds to the polymer that contains the above mentioned DOX concentration. The necrotic effect was observed using Trypan Blue staining. The results are expressed as the percentage of stained cells. Each data point was expressed as the mean of two separate experiments (mean \pm SD).

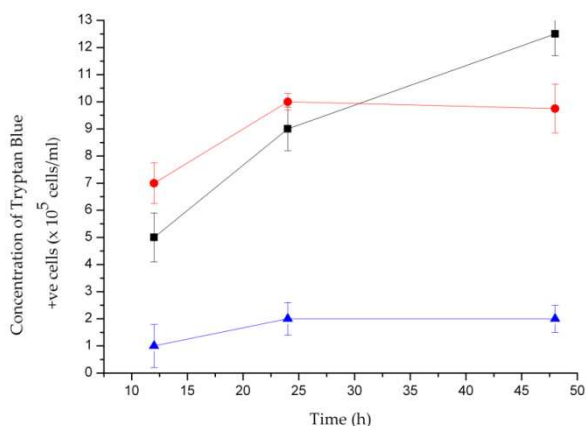


Figure 11. Treatment of MCF7 cells with Polymer (Blue), DOX-Polymer (Black) and DOX (Red) against MCF7 breast cancer cells after 12, 24 & 48 h treatment in 10 μM concentrations and the respective amount of the polymer which corresponds to the polymer that contains the above mentioned DOX concentration. The necrotic effect was observed using Trypan Blue staining. The results are expressed as the concentration of

Trypan blue + ve (stained) cells. Each data point was expressed as the mean of two separate experiments (mean \pm SD).

Conclusion

In this study, pH sensitive GMA microspheres have been synthesized aiming at creating a new material in the domain of drug delivery systems. pH responsive microcontainers with cavity inside were synthesized using Poly(Glycidyl Methacrylate) as template. These microcontainers can be used in many research fields one of which is biomedicine, as drug delivery systems. The internal cavity makes them useful candidates for drug loading and release. Acrylic Acid also helps in the loading procedure because of the carboxylic groups in the outer surface and most important, gives microcontainers the pH sensitivity. The loading and release study of the synthesized microcontainers confirms the pH responsive properties using as a model drug for this study, an anthracycline drug called DOX. The release profile of fabricated microcontainers is better at acidic than at slightly basic conditions under treatment in two different temperatures (25 and 37 $^{\circ}\text{C}$). The toxicity of the encapsulated microspheres with DOX, free DOX and the parent polymer using two specific assays, the MTT and the Trypan Blue assays, has been evaluated, aiming at determining on the one hand the cells viability and on the other hand the necrotic effect which is induced after treatment with the above mentioned compounds. Investigating the toxicity of the encapsulated DOX and the free DOX it was concluded that, in both cases, was dose depended. It is worth mentioned that the polymeric microspheres exhibit meaningless cytotoxicity among other polymeric systems according to literature.

Acknowledgements

We thank the European Research Council (ERC) for financial support of this work under the "IDEAS" project called "A Novel Micro-container drug carrier for targeted treatment of prostate cancer" with the acronym NANOTHERAPY and the reference number 232959. The authors thank Dr. Theodosios Theodosios for his contribution to the confocal experiments and his advices.

Notes and references

Dr. E.K. Efthimiadou, C. Tapeinos, Dr. N. Boukos, Dr. G. Kordas, NCSR "Demokritos Sol-Gel Laboratory, Institute for Advanced Materials, Physicochemical properties, Nanotechnology and Microsystems 153 10 Aghia Paraskevi Attikis, Greece e-mail: elefth@chem.demokritos.gr

Prof. C.A. Charitidis, M. Koklioti National Technical University of Athens School of Chemical Engineering 9 Heroon, Polytechniou St., Zografos, Athens, GR-157 80, Greece

C. Tapeinos University of Patras Materials Science Department, School of Natural Sciences 26 500 Patras, Greece

* Corresponding Author

The first two authors contributed equally to this work.

†Electronic Supplementary Information (ESI) available: [Supporting information file presents DLS diagrams of size and zeta potential versus concentration and time, diagrams of Loading Capacity and encapsulation efficiency, SEM pictures of PGMA seeds treated in simulated polymerization conditions and finally a table with polar surface and size

according to the minimum energy calculations using ChemBio3D.] See
DOI: 10.1039/b000000x/

[View Online](#)

References

1. K. Sugiyama, S. Mitsuno, Y. Yasufuku and K. Shiraishi, *Chemistry Letters*, 1997, 219-220.
2. O. Soga, C. F. van Nostrum and W. E. Hennink, *Biomacromolecules*, 2004, **5**, 818-821.
3. V. Š. Karel Ulbrich, *Advanced Drug Delivery Reviews*, 2010, **62**, 150-165.
4. J. K. a. P. Kopečková, *Advanced Drug Delivery Reviews*, 2010, **62**, 122-148.
5. D. Schmaljohann, *Adv Drug Deliv Rev*, 2006, **58**, 1655-1670.
6. I. Dimitrov, B. Trzebicka, A. H. E. Muller, A. Dworak and C. B. Tsvetanov, *Progress in Polymer Science*, 2007, **32**, 1275-1343.
7. M. Hruby, C. Konak, J. Kucka, M. Vetric, S. K. Filippov, D. Vetricka, H. Mackova, G. Karlsson, K. Edwards, B. Rihova and K. Ulbrich, *Macromol Biosci*, 2009, **9**, 1016-1027.
8. S. H. Yuk, S. H. Cho and S. H. Lee, *Macromolecules*, 1997, **30**, 6856-6859.
9. Y. M. Chen Yanfeng, *Radiation Physics and Chemistry*, 2001, **61**, 65-68.
10. B. Wang, X. D. Xu, Z. C. Wang, S. X. Cheng, X. Z. Zhang and R. X. Zhuo, *Colloids and surfaces. B, Biointerfaces*, 2008, **64**, 34-41.
11. J. E. Chung, M. Yokoyama and T. Okano, *J CONTROL RELEASE*, 2000, **65**, 93-103.
12. J. F. Chen, H. M. Ding, J. X. Wang and L. Shao, *Biomaterials*, 2004, **25**, 723-727.
13. C. J. Lee, J. S. Kang, M. S. Kim, K. P. Lee and M. S. Lee, *B Kor Chem Soc*, 2004, **25**, 1211-1216.
14. T. Basinska, *Macromol Biosci*, 2005, **5**, 1145-1168.
15. Y. Chan, V. Bulmus, M. H. Zareie, F. L. Byrne, L. Barner and M. Kavallaris, *J CONTROL RELEASE*, 2006, **115**, 197-207.
16. Z. Li, S. A. Xu, L. X. Wen, F. Liu, A. Q. Liu, Q. Wang, H. Y. Sun, W. Yu and J. F. Chen, *J CONTROL RELEASE*, 2006, **111**, 81-88.
17. Y. Hu, T. Litwin, A. R. Nagaraja, B. Kwong, J. Katz, N. Watson and D. J. Irvine, *Nano letters*, 2007, **7**, 3056-3064.
18. J. Zhang and R. D. Misra, *Acta biomaterialia*, 2007, **3**, 838-850.
19. G. L. Li, X. Y. Yang, B. Wang, J. Y. Wang and X. L. Yang, *Polymer*, 2008, **49**, 3436-3443.
20. J. F. Mano, *Advanced Engineering Materials*, 2008, **10**, 515-527.
21. J. Gao, H. Gu and B. Xu, *Accounts of chemical research*, 2009, **42**, 1097-1107.
22. X. Yang, L. Chen, B. Huang, F. Bai and X. Yang, *Polymer*, 2009, **50**, 3556-3563.
23. X. Yang, L. Chen, B. Han, X. Yang and H. Duan, *Polymer*, 2010, **51**, 2533-2539.
24. A. Chatzipavlidis, P. Bilalis, E. K. Efthimiadou, N. Boukos and G. C. Kordas, *Langmuir*, 2011, **27**, 8478-8485.
25. P. Bilalis, A. Chatzipavlidis, L.-A. Tziveleka, N. Boukos and G. Kordas, *Journal of Materials Chemistry*, 2012, **22**, 13451.
26. P. Bilalis, E. K. Efthimiadou, A. Chatzipavlidis, N. Boukos and G. C. Kordas, *Polymer International*, 2012, **61**, 888-894.
27. L. A. T. E.K. Efthimiadou, P. Bilalis, G. Kordas, *International Journal of Pharmaceutics*, 2012, **428**, 134-142.
28. R. Lehner, X. Wang, M. Wolf and P. Hunziker, *J CONTROL RELEASE*, 2012, **161**, 307-316.
29. R. Krishnan and K. S. V. Srinivasan, *Macromolecules*, 2004, **37**, 3614-3622.
30. E. Pollert, K. Knížek, M. Maryško, K. Závěta, A. Lančok, J. Boháček, D. Horák and M. Babič, *Journal of Magnetism and Magnetic Materials*, 2006, **306**, 241-247.
31. N. Hantzschel, F. Zhang, F. Eckert, A. Pich and M. A. Winnik, *Langmuir*, 2007, **23**, 10793-10800.
32. D. Horák, E. Petrovský, A. Kapička and T. Frederichs, *Journal of Magnetism and Magnetic Materials*, 2007, **311**, 500-506.
33. C. T. E. K. Efthimiadou, P. Bilalis, G. Kordas, *J Nanopart Res*, 2011, **13**, 6725-6736.
34. H. Lv, Q. Lin, K. Zhang, K. Yu, T. Yao, X. Zhang, J. Zhang and B. Yang, *Langmuir*, 2008, **24**, 13736-13741.
35. Y. L. Minchao Zhang, Da Wang, Rui Yan, Shengnan Wang, Li Yang, and Wangqing Zhang, *Macromolecules*, 2011, **44**, 842-847.
36. G. Duan, C. Zhang, A. Li, X. Yang, L. Lu and X. Wang, *Nanoscale Res Lett*, 2008, **3**, 118-122.
37. G. Socrates, *Infrared and Raman Characteristic Group Frequencies: Tables and Charts*, Wiley, 2001.
38. A. N. G. Das, M. L. Coluccio, F. Gentile, P. Candeloro, G. Cojoc, C. Liberale, F. Angelis, E. Fabrizio, *Microscopy Research and Technique* 2010, **73**, 991-995
39. K. J. Mertz Elaine, in *Epoxy Resins and Composites II*, ed. K. Dušek, Springer Berlin / Heidelberg, 1986, pp. 73-112.
40. V. K. Hana Vašková, *INTERNATIONAL JOURNAL OF MATHEMATICAL MODELS AND METHODS IN APPLIED SCIENCES*, 2011, **5**, 1197-1204.
41. V. K. Hana Vašková, in *Recent Researches in Automatic Control*, WSEAS Press, Lanzarote, Canary Islands, Spain, 2011, pp. 357-361.
42. J. L. Koenig, *Applied Spectroscopy Reviews*, 1971, **4**, 233-&
43. H. W. Choi, H. J. Woo, W. Hong, J. K. Kim, S. K. Lee and C. H. Eum, *Applied Surface Science*, 2001, **169-170**, 433-437.
44. K. J. Thomas, M. Sheeba, V. P. N. Nampoori, C. P. G. Vallabhan and P. Radhakrishnan, *J Opt a-Pure Appl Op*, 2008, **10**, 1-5.
45. M. Bacquet, C. Caze, J. Laureyns and C. Bremard, *React Polym*, 1988, **9**, 147-153.
46. D. C. Drummond, O. Meyer, K. L. Hong, D. B. Kirpotin and D. Papahadjopoulos, *Pharmacological Reviews*, 1999, **51**, 691-743.
47. I. Brigger, C. Dubernet and P. Couvreur, *Advanced Drug Delivery Reviews*, 2002, **54**, 631-651.
48. J. S. A. Martin, A. Cammarata, *Physical Pharmacy*, Lea & Febiger, Philadelphia, PA, 1969.
49. H. Huang, E. Pierstorff, E. Osawa and D. Ho, *Nano letters*, 2007, **7**, 3305-3314.
50. J. C. Reijenga, L. G. Gagliardi and E. Kenndler, *Journal of chromatography. A*, 2007, **1155**, 142-145.
51. P. S. a. J. Cleverdon, *Colloids and Surfaces B: Biointerfaces*, 1985, **13**, 73-85.
52. N. V. Sastry, J. M. Sequaris and M. J. Schwuger, *Journal of Colloid and Interface Science*, 1995, **171**, 224-233.
53. P. Somasundaran and L. Huang, *Pol J Chem*, 1997, **71**, 568-582.
54. P. Somasundaran and S. Krishnakumar, *Colloid Surface A*, 1997, **123**, 491-513.
55. D. Santhiya, S. Subramanian, K. A. Natarajan and S. G. Malghan, *J Colloid Interface Sci*, 1999, **216**, 143-153.
56. E. K. Efthimiadou, H. Thomadaki, Y. Sanakis, C. P. Raptopoulou, N. Katsaros, A. Scorilas, A. Karaliota and G. Psomas, *Journal of inorganic biochemistry*, 2007, **101**, 64-73.
57. H. Thomadaki and A. Scorilas, *Annals of the New York Academy of Sciences*, 2007, **1095**, 35-44.